Chemosphere 163 (2016) 217–226

Contents lists available at ScienceDirect

Chemosphere

journal homepage: www.elsevier.com/locate/chemosphere

Single-walled carbon nanotube release affects the microbial enzyme-catalyzed oxidation processes of organic pollutants and lignin model compounds in nature

Ming Chen [a, b, c], Xiaosheng Qin [c, *], Guangming Zeng [a, b]

[a] College of Environmental Science and Engineering, Hunan University, Changsha 410082, China
[b] Key Laboratory of Environmental Biology and Pollution Control (Hunan University), Ministry of Education, Changsha 410082, China
[c] School of Civil and Environmental Engineering, Nanyang Technological University, Singapore 639798, Singapore

HIGHLIGHTS

- SWCNT release affects the peroxidase-catalyzed oxidation processes of lignin model compounds.
- Biodegradation processes of PAHs can be disturbed by the SWCNT.
- We assessed the impact of SWCNTs on the biodegradation of β-hexachlorocyclohexane mediated by haloalkane dehalogenase using molecular dynamics simulations.

ARTICLE INFO

Article history:
Received 6 June 2016
Received in revised form
30 July 2016
Accepted 5 August 2016

Handling Editor: Tamara S. Galloway

Keywords:
Enzyme-catalyzed oxidation
Biodegradation
Organic pollutant
Lignin
PAH
Carbon nanotube

ABSTRACT

The question how microbial enzyme-catalyzed oxidation processes of organic pollutants and lignin model compounds (LMCs) are affected by the release of single-walled carbon nanotube (SWCNT) into the environment remains to be addressed at the molecular level. We have, therefore concentrated the effects of SWCNT on some important properties associated with enzyme activity and function during microbial oxidation of polycyclic aromatic hydrocarbons (benzo(*a*)pyrene, acenaphthene and anthracene), LMCs (2,6-dimethoxyphenol, guaiacol and veratryl alcohol) and β-hexachlorocyclohexane, including the behaviour of water molecules, hydrogen bonds (HBs) and hydrophobic interactions (HYs) between ligand and the enzyme, and conformational dynamics in N- and C-terminus. Our study revealed that SWCNT significantly affected the behaviour of water molecules within 5 Å of both these substrates and their respective enzymes during oxidation ($p < 0.01$), by increasing or decreasing the water number near them. SWCNT tended to significantly enhance or reduce the stability of atom pairs that formed the HBs and HYs ($p < 0.01$). N- and C-terminus conformations underwent transitions between positive and negative states or between positive state or between negative state in all analyzed complexes. Significant conformational transitions were found for all C-terminus, but only for a part of N-terminus after the inclusion of the SWCNT. These results showed that SWCNT release would significantly affect the microbial enzyme-catalyzed processes of organic pollutants and LMCs in nature.

1. Introduction

The past decades have seen a significant progress in nanotechnology with wide applications (Yamada et al., 2011; Park et al., 2013; Shulaker et al., 2013; Zhang et al., 2014; Chen et al., 2016). However, such wide applications have been resulting in that nanomaterials (e.g., carbon nanotubes, CNTs) are released into the natural environment by accident and direct acting (Shvedova et al., 2012; Bhattacharya et al., 2014). Unfortunately, CNTs are expected to be persistent in nature due to their steady features (Berry et al., 2014; Flores-Cervantes et al., 2014). Also, there is evidence that CNTs are potentially toxic to living organisms and the environment (Chandrasekaran et al., 2014; Clar et al., 2015). However, up to now, the processes and mechanism for how CNTs disturb the natural environmental processes (e.g., enzyme-catalyzed oxidation) are still largely unclear.

* Corresponding author.
E-mail address: xsqin@ntu.edu.sg (X.S. Qin).

http://dx.doi.org/10.1016/j.chemosphere.2016.08.031
0045-6535/

Organic pollutants such as polycyclic aromatic hydrocarbons (PAHs) and β-hexachlorocyclohexane (β-HCH) are persistent, being difficult to completely remove in nature (Okai et al., 2013; Chen et al., 2015a). The contamination derived from them is not limited to water body, as they also can enter the soil system by direct release and leaching. Biodegradation has been identified as an effective strategy to remove PAHs and β-HCH from the environment. For example, *Trametes versicolor* laccase was found a good candidate for the oxidation of benzo(*a*)pyrene, acenaphthene and other PAHs (Torres et al., 2003). Naphthalene 1,2-dioxygenase (NDO) is capable of performing the oxidation of anthracene (Ferraro et al., 2006). Besides, haloalkane dehalogenase (Hde) is able to be utilized for the degradation of β-HCH (Okai et al., 2013). Evidently, due to wide distribution and inadequate disposal, lignin becomes waste and even pollutant in many cases (Chen et al., 2011, 2015b). The pollution problems derived from lignin accumulation and energy shortage have aroused intensive studies over the past decades in the subject of lignin biotransformation (Munk et al., 2015; Mycroft et al., 2015). Lignin structure is so complex that researchers often employ lignin model compounds (LMCs) for lignin degradation/synthesis studies, the latter being simple compounds that contain the structural units of lignin (Bu et al., 2012; Chen et al., 2015b; Deuss and Barta, 2016). Laccase, manganese peroxidase (MnP) and lignin peroxidase (LiP) have been demonstrated to be the main ligninolytic enzymes (Sánchez, 2009). The crystal structure of *Melanocarpus albomyces* laccase has been determined, consisting of three domains (A, 1–157; B, 158–341; C, 342–559) (Hakulinen et al., 2002). *M. albomyces* laccase catalyzes the oxidation of several LMCs, such as 2,6-dimethoxyphenol (DMP) (Andberg et al., 2009) and guaiacol (Kiiskinen et al., 2002). These LMCs were also reported to be the substrates of *Phanerochaete chrysosporium* MnP (Hu et al., 2009). Veratryl alcohol (belonging to LMC) was often used as the substrate for studying the properties of LiP (Ferapontova et al., 2006). The 3D structures of both MnP and LiP from *P. chrysosporium* are available in PDB database (Rose et al., 2013), such as 1YYD (Sundaramoorthy et al., 2005) for MnP and 1LLP (Choinowski et al., 1999) for LiP. Despite wide studies on enzyme-catalyzed oxidation of organic pollutants and lignin/LMCs, little research has been conducted on the effect of CNTs on their enzyme-catalyzed oxidation processes.

The oxidation of organic pollutants and lignin mediated by microbial enzymes often occurs in the environment (Sánchez, 2009; Chen et al., 2015a). CNTs have been detected in soil and water systems. If this process occurs in the CNT-polluted places, it would lead to the fact that this enzyme-catalyzed oxidation process may be disturbed by CNTs. This is because many studies show that the presence of CNTs affects the enzymatic activity and other properties (Mubarak et al., 2014; Tavares et al., 2015). In addition, CNTs themselves can be decomposed by various enzymes. It was found that the degrading efficiency of CNTs by horseradish peroxidase was very low, and that the degrading processes were slow with long half-lives (about 80 years) (Flores-Cervantes et al., 2014). Besides horseradish peroxidase, typical enzymes already known for their ability to degrade CNTs include myeloperoxidase (Kagan et al., 2010), lactoperoxidase (Bhattacharya et al., 2015), eosinophil peroxidase (Andón et al., 2013), lignin peroxidase (Chandrasekaran et al., 2014) and manganese peroxidase (Zhang et al., 2014).

Addressing the environmental problems derived from CNTs remains a great challenge. Previous studies provide little insight into whether CNT release would affect the enzyme-catalyzed oxidation processes in nature. Thus, it is still unclear how the presence of CNTs changes the contacts between various substrates and their corresponding enzymes that are the foundation of enzymatic reaction. To tackle this problem, we aim to use molecular dynamics (MD) simulations to investigate the effects of single-walled carbon nanotube (SWCNT) on the behaviour of water molecules, hydrogen bonds (HBs) and hydrophobic interactions (HYs), and conformational dynamics in N- and C-terminus during the enzyme-catalyzed oxidation of PAHs (Benzo(*a*)pyrene, acenaphthene and anthracene), lignin (lignin model compounds were used as representative, including DMP, guaiacol and veratryl alcohol), and β-HCH by comparing the conformations in the presence and absence of SWCNTs.

2. Materials and methods

2.1. Data on enzyme-catalyzed oxidation

We found enzyme-catalyzed oxidation information of organic contaminants and LMCs by searching the University of Minnesota Biocatalysis/Biodegradation Database (Gao et al., 2010), BRENDA database (Schomburg et al., 2002) and Google Scholar. Finally, we selected eight pairs of substrate-enzyme systems based on the following criteria: (1) the experimental 3D structures of enzymes must be available; (2) the substrate molecules must be small in size. These substrates and their corresponding enzymes were: laccase vs. guaiacol; LiP vs. veratryl alcohol; MnP vs. DMP; MnP vs. guaiacol; laccase vs. benzo(*a*)pyrene; laccase vs. acenaphthene; NDO vs. anthracene; Hde vs. β-HCH. For simplicity, we defined their abbreviations in Table 1.

2.2. Structure models of organic pollutants, LMCs and enzymes

Some experiment-determined 3D structures of the above selected enzymes available in RSC PDB database (Rose et al., 2013) (http://www.rcsb.org/pdb/home/home.do) enable the present study. The structures of substrate molecules were taken directly from ChemSpider (http://www.chemspider.com/) (Pence and Williams, 2010), while those of selected enzymes were downloaded from PDB with some simple treatment as described in our previous studies (Chen et al., 2011, 2015b).

2.3. Preparation of initial conformations

SWCNT-bound conformation models of the enzymes were generated using PatchDock (Schneidman-Duhovny et al., 2005), and then refined by FireDock (Mashiach et al., 2008). The model system adopted in each PatchDock run was composed of an enzyme and a SWCNT (6,6) with a length of 2 nm. Substrate molecules were docking into their corresponding enzymes with and without SWCNTs by Molegro Virtual Docker (MVD) (Thomsen and Christensen, 2006). MolDock score [Grid] was employed as the scoring function with 0.3 Å of grid resolution, whereas the selected algorithm was Moldock SE. The obtained candidates were ranked based on MolDock score and Re-Rank score to get the best pose which was selected as the final model for further studies.

2.4. MD simulations

Gromacs 4.6 packages (Pronk et al., 2013) were adopted to perform the simulations where OPLS-AA force field was employed (Kaminski et al., 2001). RESP charges of small molecules were obtained at the HF/6-31G* level. Other field parameters of small molecules were determined by MKTOP 2.0 (Ribeiro et al., 2008), a Perl script. For each pair of substrate and its corresponding enzyme, we constructed two systems, one with SWCNT and another one without SWCNT which was used as a control group with the same simulation conditions (Table 1, Figs. 1–4). Thus, a total of 16 complexes were presented. Each complex was solvated by SPC water model in two cubic boxes with the same size. 36,284–215,956

Table 1
Substrate-enzymes systems used in this study.

Substrate	Enzyme	Complex/system without SWCNT	Complex/system with SWCNT	Experiment-determined enzyme structure	Experimental evidence for enzyme-catalyzed oxidation
LMC					
Guaiacol	Laccase	Lac-Gua	SWCNT-Lac-Gua	1GW0	(Kiiskinen et al., 2002)
Veratryl alcohol	LiP	LiP-Ver	SWCNT-LiP-Ver	1LLP	(Ferapontova et al., 2006)
DMP	MnP	MnP-Dim	SWCNT-MnP-Dim	1YYD	(Hu et al., 2009)
Guaiacol	MnP	MnP-Gua	SWCNT-MnP-Gua	1YYD	(Hu et al., 2009)
PAH					
Benzo(*a*) pyrene	Laccase	Lac-Ben	SWCNT-Lac-Ben	1GYC	(Torres et al., 2003)
Acenaphthene	Laccase	Lac-Ace	SWCNT-Lac-Ace	1GYC	(Torres et al., 2003)
Anthracene	NDO	NDO-Ant	SWCNT-NDO-Ant	4HM6	(Ferraro et al., 2006)
β-HCH	Hde	Hde-Hex	SWCNT-Hde-Hex	4H77	(Okai et al., 2013)

LMC, lignin model compound; LiP, lignin peroxidise; DMP, 2,6-dimethoxyphenol; MnP, manganese peroxidise; NDO, naphthalene 1,2-dioxygenase; β-HCH, β-hexachlorocyclohexane; Hde, haloalkane dehalogenase.

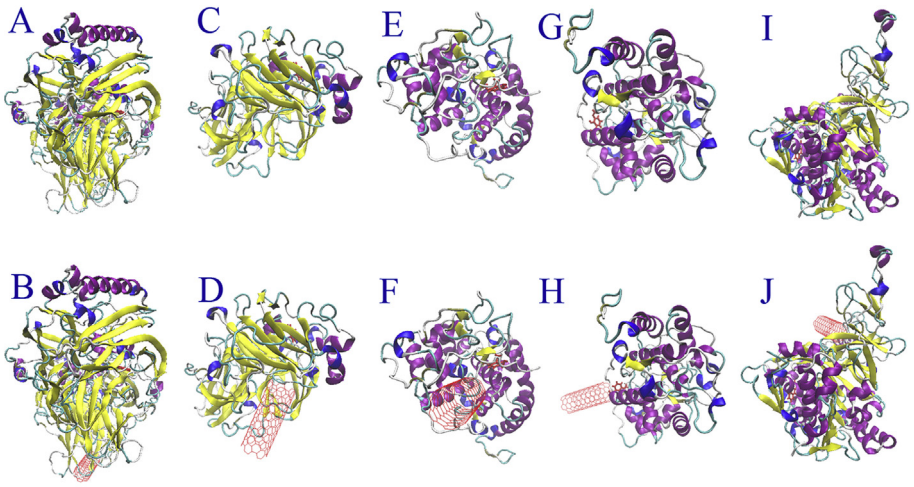

Fig. 1. Initial conformations of Lac-Gua (A), SWCNT-Lac-Gua (B), Lac-Ace (C), SWCNT-Lac-Ace (D), LiP-Ver (E), SWCNT-LiP-Ver (F), MnP-Dim (G), SWCNT-MnP-Dim (H), NDO-Ant (I) and SWCNT-NDO-Ant (J).

atoms and 10,482–66,321 water molecules were found in these boxes (Table S1). System neutrality was achieved by adding Na^+ or Cl^-. Then, steepest descent minimization was completed. The systems are subjected to restraining forces on SWCNTs, substrate molecules and degrading enzymes in SWCNT bound systems and on substrate molecules and degrading enzymes in SWCNT free systems. Subsequently, the equilibration was run in both 300 ps of NVT ensemble and 300 ps of NPT ensemble. Finally, we performed 30-ns MD simulations for SWCNT-MnP-Gua, MnP-Gua, SWCNT-Lac-Ben, Lac-Ben, SWCNT-Hde-Hex and Hde-Hex, respectively, using Particle Mesh Ewald for the calculation of long-range electrostatic interactions (Darden et al., 1993), with a 2 fs of time step. For each of the remaining systems, we carried out 10-ns MD simulations.

2.5. Water number

The number of water molecules within 5 Å of degrading enzymes and within 5 Å of substrate molecules during biodegradation was calculated by customized tcl script in VMD (Humphrey et al., 1996).

2.6. Identification of HBs and HYs

First, HBs and HYs in initial SWCNT free complexes were identified by programme the protein-ligand interaction profiler (PLIP; https://projects.biotec.tu-dresden.de/plip-web/plip/index) (Salentin et al., 2015). In the next step, we monitored the changes of these interactions during the entire simulation using the customized tcl script in VMD.

2.7. Dihedrals for N- and C-terminus

For simplicity, we described the conformational changes in N- and C-terminus using the C_α-dihedrals of the first four residues and named them N-ter-dihedral and C-ter-dihedral, respectively. Subsequently, we monitored the changes of these two dihedrals in all analyzed systems over time.

2.8. Statistical analyses

For all of the above organic pollutants, LMCs and their enzymes, statistical difference ($\alpha = 0.05$) in water number, LHBs, HDs, N-ter-dihedral and C-ter-dihedral between each pair of complexes with and without SWCNT was determined by two-tailed *t*-test, respectively.

3. Results

3.1. Behaviour of water molecules

In this study, we described the behaviour of water molecules by

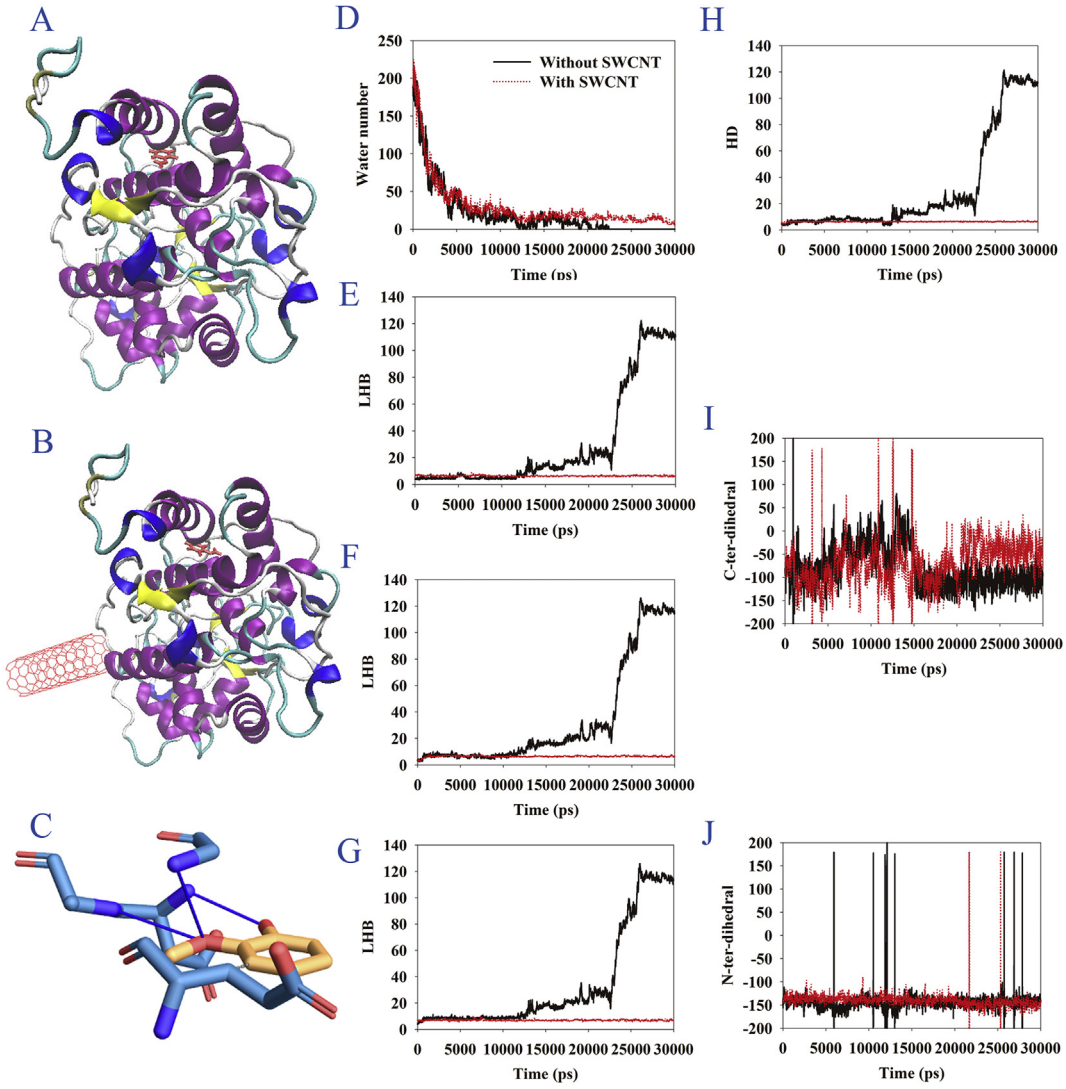

Fig. 2. Conformational dynamics and interactional changes in MnP-Gua with and without SWCNT and water number distribution. A, Initial conformation of MnP-Gua; B, Initial conformation of SWCNT-MnP-Gua; C, interactions between MnP and guaial in the initial conformation; D, water number; E, GLY34:N/Guaial:O1, 475_5162_hb; F, ASP36:N/Guaial:O2, 497_5169_hb; G, ALA37:N/Guaial:O1, 509_5162_hb; H, GLU32:CB/Guaial:C3, 5164_454_hy; I, C-ter-dihedral; J, N-ter-dihedral.

calculating the changes in number of water molecules within 5 Å of the enzymes and within 5 Å of their substrate molecules during biodegradation. For simplicity, we called this region "5 Å region". Thus, if not explicitly stated, the water number refers to that within this 5 Å region.

The amount of water molecules was significantly different in CNT-bound MnP-Gua systems from that in CNT free MnP-Gua systems ($t = -50.3$, $p < 0.01$). In the initial stage of the simulation, these two systems had similar numbers of water molecules (Fig. 2D). Moreover, water number gradually decreased in these two systems. After 20 ns, the water number had become zero in MnP-Gua system; however, in SWCNT-MnP-Gua system, the water number ranged from 6 to 25. These findings indicated that the presence of SWCNT changed the behaviour of water molecules. To further confirm whether this rule applies to other systems composed of LMCs and ligninolytic enzymes, we investigated the behaviour of water molecules in Lac-Gua, LiP-Ver and MnP-Dim systems with and without SWCNTs. The average water numbers were 51 and 47 in SWCNT-Lac-Gua and Lac- Gua ($t = -7.4$, $p < 0.01$), respectively (Fig. S1A). The average number of water molecules in SWCNT-LiP-Ver was smaller than that in LiP-Ver (59 vs. 76, $t = 38.8$, $p < 0.01$) (Fig. S2A). For MnP and DMP (Fig. S3A), the inclusion of SWCNT significantly decreased the water number in MnP-Dim (average water number decreased from 45 to 33; $t = 21.9$, $p < 0.01$).

In order to study the effect of SWCNT on water behaviour adjacent to PAHs and their degrading enzymes, we first selected laccase and benzo(*a*)pyrene for this purpose, and then constructed SWCNT bound and free systems (Fig. 3A and B). For each of these two systems, we performed a 30-ns simulation. Water numbers in the 5 Å regions of these two systems experienced a downward trend over this time and were significantly different ($t = -40.5$, $p < 0.01$) (Fig. 3D). Before 15 ns, the water number in SWCNT bound complex was sometimes larger and sometimes smaller than that in SWCNT free complex. However, after 15 ns, the water number in CNT bound complex was generally larger than that in CNT free complex, although some exceptions were found. Subsequently, we analyzed the water behaviour in complexes composed of other PAHs (including acenaphthene and anthracene) and their respective degrading enzymes. It was found that the mean water number in the 5 Å region of Lac-Ace was nearly equal to that in SWCNT-Lac-Ace (34 vs. 36, $t = -4.8$, $p < 0.01$) (Fig. S4A). Interestingly, the inclusion of SWCNT significantly decreased the water number in the

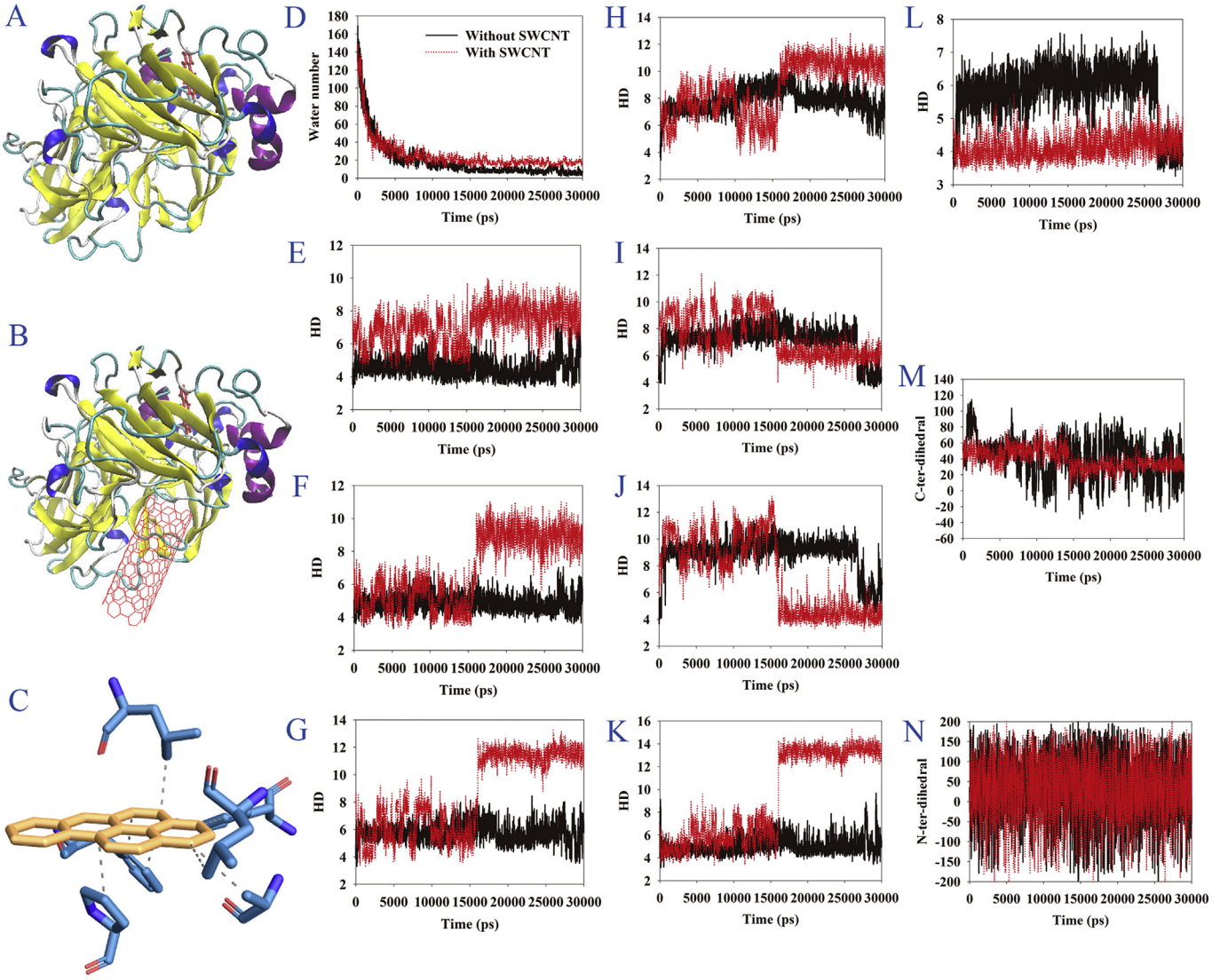

Fig. 3. Conformational dynamics and interactional changes in Lac-Ben with and without SWCNT and water number distribution. A, Initial conformation of Lac-Ben; B, Initial conformation of SWCNT- Lac-Ben; C, interactions between laccase and benzo(*a*)pyrene in the initial conformation; D, water number; E, PHE344:CD2/Benzo(*a*)pyrene:C11, 7473_5173_hy; F, PHE344:CE2/Benzo(*a*)pyrene:C13, 7475_5177_hy; G, PHE450:CZ/Benzo(*a*)pyrene:C13, 7475_6732_hy; H, LEU459:CD1/Benzo(*a*)pyrene:C13, 7475_6877; I, ALA80:CB/Benzo(*a*)pyrene:C14, 7476_1178_hy; J, LEU112:CD1/Benzo(*a*)pyrene:C14, 7476_1668; K, PHE450:CE2/Benzo(*a*)pyrene:C15, 7477_6730_hy; L, PRO346:CG/Benzo(*a*)pyrene:C3, 7465_5203_hy; M, C-ter-dihedral; N, N-ter-dihedral.

5 Å region of NDO-Ant complex ($t = 40.2$, $p < 0.01$) (Fig. S5A), although there was a similar number of water molecules in SWCNT bound and free complexes in the early stage of the experiment.

Water number exhibited significantly different patterns between Hde-Hex and SWCNT-Hde-Hex systems ($t = 6.0$, $p < 0.01$) (Fig. 4D). Noteworthy, the water number was very small in these two complexes. In the later period of the experiment, water number was comparable in these two complexes.

3.2. Conformational dynamics in N- and C-terminus

To observe and compare conformational transition features of N- and C-terminus with and without SWCNT, we defined two new variables N-ter-dihedral and C-ter-dihedral (See Materials and methods). When N-ter-dihedral or C-ter-dihedral was negative, we termed N-terminus or C-terminus was at a negative state. Otherwise, they were at a positive state.

As depicted in Fig. 2I and J, the maximum fluctuation ranges for N-ter-dihedral and C-ter-dihedral were similar between MnP-Gua and SWCNT-MnP-Gua complexes. However, C-terminus conformations in these two complexes frequently varied between negative and positive states, while N-terminus conformation at a positive state only occasionally appeared within 30 ns. C-terminus conformation was very unstable in Lac-Gua (Fig. S1F). By contrast, it was quickly stabilized in SWCNT-Lac-Gua. In most of the time, C-terminus conformations only varied between the negative states. N-terminus transition between ~−170°−−160° and ~160°−170° in these two complexes (Fig. S1G). The change rule for N- and C-terminus conformations in LiP-Ver and SWCNT-LiP-Ver was almost opposite to that in Lac-Gua complexes with and without SWCNT (Fig. S2H and I). That is, N-terminus transformed between a type of state (negative state) and C-terminus transformed between two types of states. We did not observe the stability of C-terminus conformation in MnP-Dim upon SWCNT binding; C-terminus conformation still dramatically changed in MnP (Fig. S3G). N-terminus conformation was relatively stable in MnP-Dim and SWCNT-MnP-Dim, because it fluctuated within a narrow range (Fig. S3H).

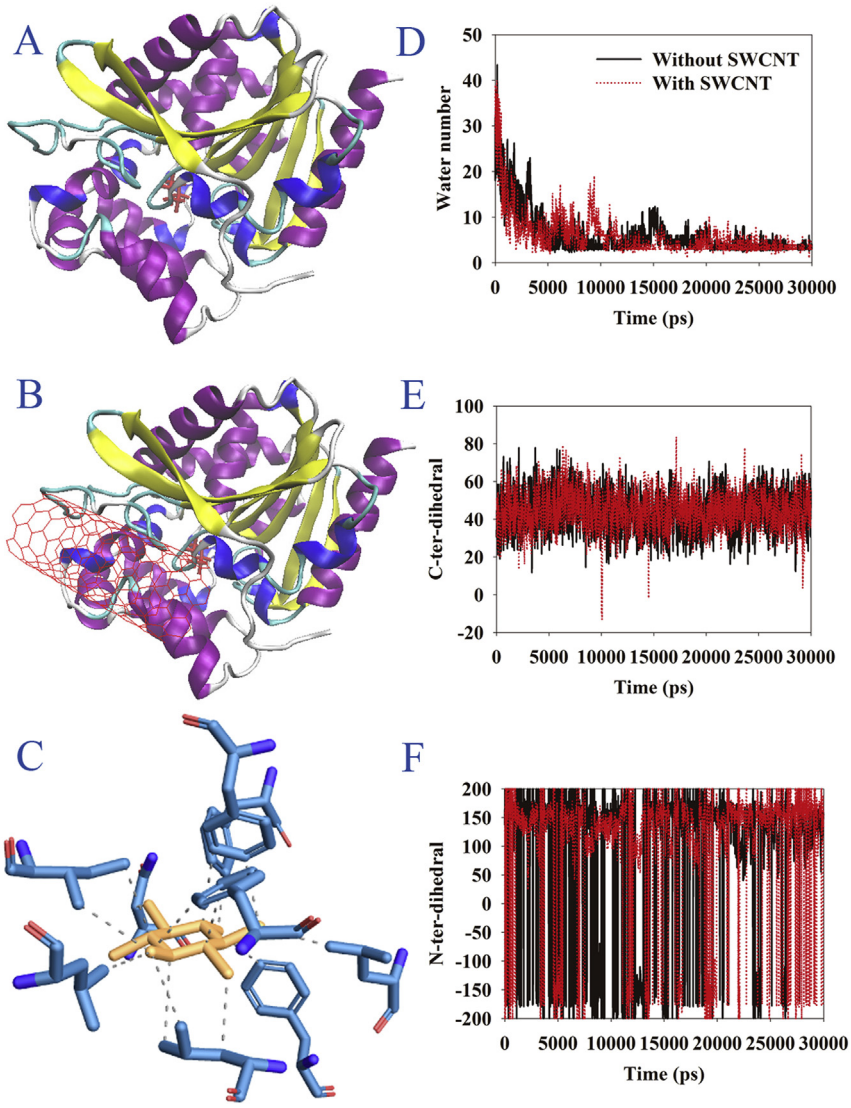

Fig. 4. Initial conformations of Hde-Hex (A) and SWCNT-Hde-Hex (B), initial interactions between Hde and β-HCH (C), water number distribution (D), C-ter-dihedral (E) and N-ter-dihedral (F).

Conformational dynamics in N- and C-terminus during oxidation of PAHs were also investigated. In SWCNT-Lac-Ben, mean N-ter-dihedral and C-ter-dihedral were 30° and 40° respectively, which were smaller than those in the SWCNT free complex Lac-Ben, respectively (Fig. 3M and N). Smaller dihedrals observed in SWCNT-Lac-Ben were due to that SWCNT disrupted the native conformation of N- and C-terminus. C-terminus conformation frequently fluctuated with significant different C-ter-dihedrals in both Lac-Ace and SWCNT-Lac-Ace ($p < 0.01$) (Fig. S4H), and their N-ter-dihedrals varied in a wide range between −0.1°–−178° and 0.3°–178° (Fig. S4I). C-terminus conformation in NDO-Ant binding to SWCNT still maintained a stable state, and slightly varied around ~−120°–−130° (Fig. S5D). We further examined N-terminus conformational dynamics in NDO-Ant with and without SWCNT, showing that N-terminus conformation changed between negative and positive states, regardless of the presence of SWCNT (Fig. S5E).

Varying pattern in C-terminus conformation in Hde-Hex complex was changed when bound to SWCNT ($p < 0.05$) (Fig. 4E), while N-terminus conformation fast shifted between positive and negative states as a function of time in Hde-Hex complex (Fig. 4F).

3.3. Changes in HBs and HYs

In the following section, we presented the effects of SWCNT on the contacts between enzymes and their substrates. For convenience, we defined the atom-atom distance for a HY as hydrophobic distance (HD).

In the initial conformations, LMCs formed HBs and/or HYs with their corresponding enzymes, including 3 HBs and 1 HYs for MnP-Gua (Fig. 2), 2 HBs and 2 HYs for Lac-Gua (Fig. S1), 3 HBs and 3 HYs for LiP-Ver (Fig. S2) and 2 HBs and 3 HYs for MnP-Dim (Fig. S3). All these interactions were monitored under the conditions with and without the SWCNT. The length of HB (LHB) or HD for most of these interactions except for 5169_2910_hy showed significant differences between all SWCNT bound and free complexes ($p < 0.01$), respectively. This observation meant that SWCNT had significant effects on the contacts between LMCs and their corresponding enzymes during the enzyme-catalyzed oxidation. The native contacts between them were not kept due to the appearance of SWCNTs, which would disturb the normal oxidation processes. LHBs for 475_5162_hb, 497_5169_hb and 509_5162_hb and HD for 5164_454_hy sharply varied with time in MnP-Gua, but were well

equilibrated after the inclusion of SWCNT (Fig. 2). 12006_16987_hb and 16985_11125_hy were quickly disrupted after the beginning of the simulation in Lac-Gua systems with and without SWCNT; 11076_16980_hb disappeared from the start and appeared at about 5 ps, 10 ps, 89–90 ps and 130–150 ps in SWCNT free complex; compared with the SWCNT free complex, 11076_16980_hb appeared for a longer time in SWCNT bound complex during the simulations. 16984_11104_hy was not found in SWCNT free Lac-Gua complex after the simulation had begun; SWCNT tried to maintain this hydrophobic interaction in Lac-Gua, but finally failed. This was because 16984_11104_hy was completely disrupted in Lac-Gua at the later period (Fig. S1). Interestingly, the SWCNT seemed to enhance the moving ability of atoms involved in the HBs and HYs between LiP and veratryl alcohol, because these interactions were generally more unstable in SWCNT bound complex than in SWCNT free complex (Fig. S2). HBs and HYs between MnP and DMP were quickly broken, but the LHBs and HDs were fast stabilized. In the presence of SWCNT, these LHBs and HDs showed a staircase-like increasing (Fig. S3).

The analyzed interactions between PAHs and their degrading enzymes were 0 HBs and 8 HYs for Lac-Ben (Fig. 3), 0 HBs and 6 HYs for Lac-Ace (Fig. S4), and 0 HBs and 2 HYs for NDO-Ant (Fig. S5). Their stability was evaluated. All these interactions were significantly different between SWCNT bound and free complexes ($p < 0.05$), respectively. Consistent with the oxidation of LMCs, PAH oxidation processes were also significantly affected by SWCNTs; however, no HBs were observed between PAHs and their degrading enzymes. The HD for 7473_5173_hy was generally larger in SWCNT-Lac-Ben than that in Lac-Ben. Furthermore, 7473_5173_hy had been completely disrupted in SWCNT-Lac-Ben (Fig. 3). The HDs for 7475_5177_hy, 7475_6732_hy and 7477_6730_hy were stable under the condition without the SWCNT but had a staircase-like increasing in the presence of the SWCNT. For the rest interactions, the SWCNT tended to make the HDs close to or smaller than those in SWCNT-Lac-Ben, respectively. In Lac-Ace with or without the SWCNT, 7465_1668_hy, 7466_5203_hy, 7470_1178_hy, 7471_5173_hy, 7471_6877_hy and 7472_6730_hy were unstable during the whole simulations (Fig. S4). The HDs for 9971_5512_hy and 9976_8496_hy in NDO-Ant first increased for some time, and then decreased; finally, they were stabilized and slightly fluctuated around 4.5 Å (Fig. S5). Overall, these HDs were larger in SWCNT-NDO-Ant than in NDO-Ant, especially for 9971_5512_hy. The mean distance for 9971_5512_hy was 5.7 Å in the absence of SWCNT and was 10.6 Å in the presence of SWCNT.

The β-HCH, an isomer of insecticide lindane γ-HCH, is of special concern due to its persistence, toxicity and bioaccumulation (Okai et al., 2013). It can be effectively degraded by Hde. For the complexes composed of Hde and β-HCH with and without SWCNT, fourteen HYs were monitored over time (Fig. 5). The HDs for 4611_573_hy, 4612_2142_hy, 4612_3310_hy, 4612_3858_hy, 4613_2637_hy, 4614_2758_hy and 4615_3853_hy in SWCNT bound complex fast reached equilibrium, and fluctuated around 4 Å which is the allowed maximum distance of carbon atoms for a given HY in PLIP (Salentin et al., 2015); these HYs in SWCNT free complex were already completely broken at the later period of the simulation. For other seven HYs, HDs were generally larger than 4 Å in both SWCNT bound and free complexes, implying that they had been disrupted during the simulations. However, it should be noted that most of these HDs except for 4610_3314_hy were significantly different between SWCNT bound and free complexes, respectively ($p < 0.01$).

4. Discussion

CNTs will be inevitably released into the environment due to increasing use in various fields (Flores-Cervantes et al., 2014; Clar et al., 2015). Studies on the environmental consequences of CNTs are still very scarce, even though CNTs have been identified as a potential threat to human health and the environment (Chen et al., 2016). How the release of CNTs impacts the enzyme-catalyzed oxidation processes of organic pollutants and lignin is still an unsolved problem today. Therefore, we first collected the enzyme-catalyzed oxidation information on various organic pollutants and lignin from several sources. Due to high complexity and unavailability of lignin structure, to be consistent with the previous studies (Bu et al., 2012; Chen et al., 2015b; Deuss and Barta, 2016), we employed LMCs as representative. Taking data representative and the availability of experiment-determined 3D structures of the enzymes into consideration, eight pairs of substrates and their enzymes were adopted (Table 1). Then, MD simulation was performed for each complex. MD simulations have been shown to have great advantages in examining the trajectory of molecular motions (Sun et al., 2013; He et al., 2015) and they have been particularly helpful in understanding the biodegradation processes of lignin (Chen et al., 2011, 2015b), nitrile (Zhang et al., 2013), cellulose (Liu et al., 2012) and CNTs (Chen et al., 2016). The SWCNT release significantly affected the enzyme-catalyzed oxidation processes of organic contaminants and LMCs in nature by changing the behaviour of water molecules, disrupting the HBs and HYs between substrates and their enzymes and transforming the conformations of N- and C-terminus, etc.

Water molecules play a critical role in protein functions and the interaction of protein with ligands (Cappel et al., 2011; Kitjaruwankul et al., 2015; Yuan et al., 2015). Our results showed that water number was significantly different between CNT bound and free systems for all analyzed organic pollutants, LMCs and their corresponding enzymes, suggesting that the incorporation of SWCNTs affected the behaviour of water molecules during the enzyme-catalyzed oxidation. The change in water molecule behaviour as reflected by water number would influence the binding of these substrates to their corresponding enzymes, such as binding modes and the complex structures (Li and Lazaridis, 2007; Cappel et al., 2011).

Not all of N-terminus conformations were significantly affected by the SWCNT. By contrast, C-terminus conformations were significantly disturbed in all analyzed complexes ($p < 0.05$). This finding implied that SWCNTs could be used as a tool for targeted regulation of C-terminus conformation and further enzyme activity. Moreover, an interesting phenomenon was that C-terminus conformations often transformed between a type of state (positive or negative), while N-terminus conformations preferred to change between positive and negative states, although some exceptions were also presented.

LMCs, PAHs and β-HCH could form HBs and/or HYs with their corresponding enzymes during oxidation. Our previous study showed that the most abundant interaction way was HYs between ligninolytic enzymes and the ligand lignin derivative (Chen et al., 2011). Moreover, it has been demonstrated by us that HYs were necessary to the interaction of laccase with LMCs and HBs were also often found between them although not all (Chen et al., 2015b). All these previous studies implied that the interactions between substrate and enzyme were important for the oxidation of LMCs/lignin. Thus, interactional changes between LMCs and their corresponding enzymes which were found due to the appearance of SWCNTs in the present study may lead to the changes in the enzyme-catalyzed oxidation processes of LMCs/lignin. Microbial degradation has been known to be the main process for PAH degradation (Haritash and Kaushik, 2009). Natural biodegradation processes of PAHs were influenced by many factors (Johnsen et al., 2005), including bioavailability, microbial activity, etc. Our study

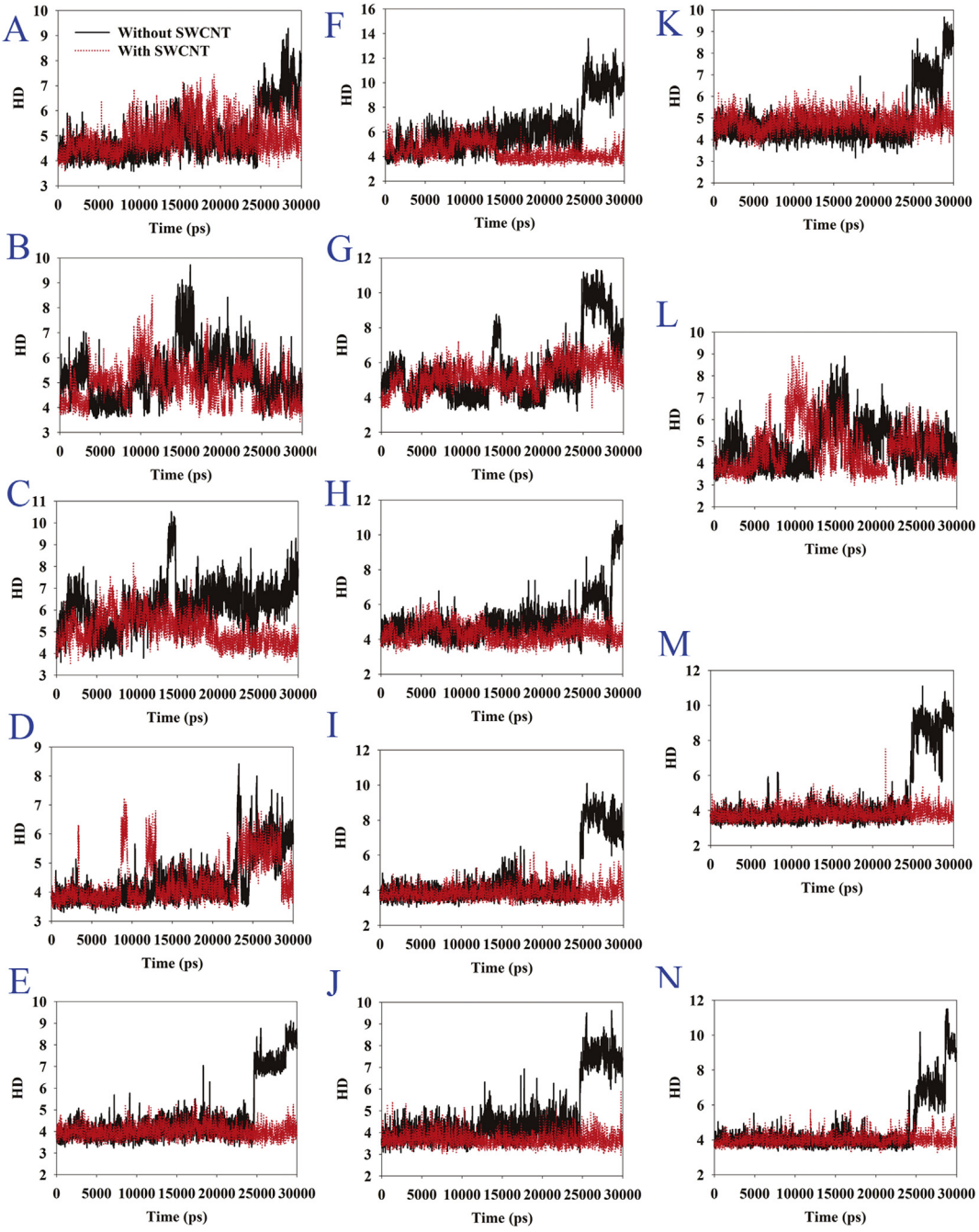

Fig. 5. Interactional changes in Hde-Hex with and without SWCNT. A, LEU248:CD2/β-HCH:C5, 4609_3862_hy; B, PHE151:CE2/β-HCH:C2, 4606_2360_hy; C, PHE143:CZ/β-HCH:C4, 4608_2229_hy; D, ILE211:CD/β-HCH:C6, 4610_3314_hy; E, ASN38:CB/β-HCH:Cl1, 4611_573_hy; F, LEU138:CD1/β-HCH:Cl2, 4612_2142_hy; G, PHE143:CE1/β-HCH:Cl2, 4612_2225_hy; H, ILE211:CG2/β-HCH:Cl2, 4612_3310_hy; I, LEU248:CD1/β-HCH:Cl2, 4612_3858_hy; J, PHE169:CE1/β-HCH:Cl3, 4613_2637_hy; K, PHE273:CZ/β-HCH:Cl3, 4613_4259_hy; L, PHE151:CZ/β-HCH:Cl4, 4614_2362_hy; M, LEU177:CD1/β-HCH:Cl4, 4614_2758_hy; N, LEU248:CB/β-HCH:Cl5, 4615_3853_hy.

showed, besides these known factors, in the case of SWCNT contamination, SWCNT would significantly disturb the contacts between PAHs and degrading enzymes, which further made the biodegradation process becoming more complicated. Moreover, attention should be paid to the combined toxicity of PAHs and CNTs, because all of them presented toxic effects on living organisms and the nature (Clar et al., 2015; Zoppini et al., 2016). For the complexes composed of Hde and β-HCH with and without SWCNT, we monitored the HD variations for fourteen HYs over time. It was found that thirteen HDs were significantly disturbed by the SWCNTs ($p < 0.01$).

When we brought all these results together, we could conclude that the SWCNT significantly disturbed the interactions between substrates and their enzymes by affecting water molecular behaviour, HYs, HBs and N- and C-terminus conformations, and thus would influence the native enzyme-catalyzed oxidation processes of these substrates, including organic pollutants and lignin/LMCs. The contacts between substrates and their enzymes are vital to occurrence of enzymatic reactions. Changes in these contacts, thus, might affect the activity and function of the enzymes during their oxidation.

Acknowledgments

The study was financially supported by the National Natural Science Foundation of China (51508177, 51521006), the Program for Changjiang Scholars and Innovative Research Team in University (IRT-13R17) and the Fundamental Research Funds for the Central Universities.

Appendix A. Supplementary data

Supplementary data related to this article can be found at http://dx.doi.org/10.1016/j.chemosphere.2016.08.031.

References

Andón, F.T., Kapralov, A.A., Yanamala, N., Feng, W., Baygan, A., Chambers, B.J., Hultenby, K., Ye, F., Toprak, M.S., Brandner, B.D., 2013. Biodegradation of single-walled carbon nanotubes by eosinophil peroxidase. Small 9, 2721–2729.

Andberg, M., Hakulinen, N., Auer, S., Saloheimo, M., Koivula, A., Rouvinen, J., Kruus, K., 2009. Essential role of the C-terminus in *Melanocarpus albomyces* laccase for enzyme production, catalytic properties and structure. Febs J. 276, 6285–6300.

Berry, T.D., Filley, T.R., Blanchette, R.A., 2014. Oxidative enzymatic response of white-rot fungi to single-walled carbon nanotubes. Environ. Pollut. 193, 197–204.

Bhattacharya, K., El-Sayed, R., Andón, F.T., Mukherjee, S.P., Gregory, J., Li, H., Zhao, Y., Seo, W., Fornara, A., Brandner, B., 2015. Lactoperoxidase-mediated degradation of single-walled carbon nanotubes in the presence of pulmonary surfactant. Carbon 91, 506–517.

Bhattacharya, K., Sacchetti, C., El-Sayed, R., Fornara, A., Kotchey, G.P., Gaugler, J.A., Star, A., Bottini, M., Fadeel, B., 2014. Enzymatic 'stripping' and degradation of PEGylated carbon nanotubes. Nanoscale 6, 14686–14690.

Bu, Q., Lei, H., Zacher, A.H., Wang, L., Ren, S., Liang, J., Wei, Y., Liu, Y., Tang, J., Zhang, Q., 2012. A review of catalytic hydrodeoxygenation of lignin-derived phenols from biomass pyrolysis. Bioresour. Technol. 124, 470–477.

Cappel, D., Wahlström, R., Brenk, R., Sotriffer, C.A., 2011. Probing the dynamic nature of water molecules and their influences on ligand binding in a model binding site. J. Chem. Inf. Model. 51, 2581–2594.

Chandrasekaran, G., Choi, S.-K., Lee, Y.-C., Kim, G.-J., Shin, H.-J., 2014. Oxidative biodegradation of single-walled carbon nanotubes by partially purified lignin peroxidase from *Sparassis latifolia* mushroom. J. Ind. Eng. Chem. 20, 3367–3374.

Chen, M., Qin, X., Li, J., Zeng, G., 2016. Probing molecular basis of single-walled carbon nanotube degradation and nondegradation by enzymes based on manganese peroxidase and lignin peroxidase. RSC Adv. 6, 3592–3599.

Chen, M., Xu, P., Zeng, G., Yang, C., Huang, D., Zhang, J., 2015a. Bioremediation of soils contaminated with polycyclic aromatic hydrocarbons, petroleum, pesticides, chlorophenols and heavy metals by composting: applications, microbes and future research needs. Biotechnol. Adv. 33, 745–755.

Chen, M., Zeng, G., Tan, Z., Jiang, M., Li, H., Liu, L., Zhu, Y., Yu, Z., Wei, Z., Liu, Y., Xie, G., 2011. Understanding lignin-degrading reactions of ligninolytic enzymes: binding affinity and interactional profile. PLoS One 6, e25647.

Chen, M., Zeng, G.M., Lai, C., Li, J., Xu, P., Wu, H.P., 2015b. Molecular basis of laccase bound to lignin: insight from comparative studies on the interaction of *Trametes versicolor* laccase with various lignin model compounds. Rsc Adv. 5, 52307–52313.

Choinowski, T., Blodig, W., Winterhalter, K.H., Piontek, K., 1999. The crystal structure of lignin peroxidase at 1.70 angstrom resolution reveals a hydroxy group on the C-beta of tryptophan 171: a novel radical site formed during the redox cycle. J. Mol. Biol. 286, 809–827.

Clar, J.G., Gustitus, S.A., Youn, S., Silvera Batista, C.A., Ziegler, K.J., Bonzongo, J.C.J., 2015. Unique toxicological behavior from single-wall carbon nanotubes separated via selective adsorption on hydrogels. Environ. Sci. Technol. 49, 3913–3921.

Darden, T., York, D., Pedersen, L., 1993. Particle Mesh Ewald – an N.Log(N) method for Ewald sums in large systems. J. Chem. Phys. 98, 10089–10092.

Deuss, P.J., Barta, K., 2016. From models to lignin: transition metal catalysis for selective bond cleavage reactions. Coord. Chem. Rev. 306, 510–532.

Ferapontova, E.E., Castillo, J., Gorton, L., 2006. Bioelectrocatalytic properties of lignin peroxidase from *Phanerochaete chrysosporium* in reactions with phenols, catechols and lignin-model compounds. Biochim. Biophys. Acta (BBA) Gen. Subj. 1760, 1343–1354.

Ferraro, D.J., Okerlund, A.L., Mowers, J.C., Ramaswamy, S., 2006. Structural basis for regioselectivity and stereoselectivity of product formation by naphthalene 1, 2-dioxygenase. J. Bacteriol. 188, 6986–6994.

Flores-Cervantes, D.X., Maes, H.M., Schäffer, A., Hollender, J., Kohler, H.-P.E., 2014. Slow biotransformation of carbon nanotubes by horseradish peroxidase. Environ. Sci. Technol. 48, 4826–4834.

Gao, J., Ellis, L.B., Wackett, L.P., 2010. The University of Minnesota biocatalysis/biodegradation database: improving public access. Nucleic Acids Res. 38, D488–D491.

Hakulinen, N., Kiiskinen, L.-L., Kruus, K., Saloheimo, M., Paananen, A., Koivula, A., Rouvinen, J., 2002. Crystal structure of a laccase from *Melanocarpus albomyces* with an intact trinuclear copper site. Nat. Struct. Mol. Biol. 9, 601–605.

Haritash, A., Kaushik, C., 2009. Biodegradation aspects of polycyclic aromatic hydrocarbons (PAHs): a review. J. Hazard. Mater. 169, 1–15.

He, G., Zhang, M., Zhou, Q., Pan, G., 2015. Molecular dynamics simulations of structural transformation of perfluorooctane sulfonate (PFOS) at water/rutile interfaces. Chemosphere 134, 272–278.

Hu, M., Zhang, W., Wu, Y., Gao, P., Lu, X., 2009. Characteristics and function of a low-molecular-weight compound with reductive activity from Phanerochaetechrysosporium in lignin biodegradation. Bioresour. Technol. 100, 2077–2081.

Humphrey, W., Dalke, A., Schulten, K., 1996. VMD: visual molecular dynamics. J. Mol. Graph. 14, 33–38.

Johnsen, A.R., Wick, L.Y., Harms, H., 2005. Principles of microbial PAH-degradation in soil. Environ. Pollut. 133, 71–84.

Kagan, V.E., Konduru, N.V., Feng, W., Allen, B.L., Conroy, J., Volkov, Y., Vlasova, I.I., Belikova, N.A., Yanamala, N., Kapralov, A., 2010. Carbon nanotubes degraded by neutrophil myeloperoxidase induce less pulmonary inflammation. Nat. Nanotechnol. 5, 354–359.

Kaminski, G.A., Friesner, R.A., Tirado-Rives, J., Jorgensen, W.L., 2001. Evaluation and reparametrization of the OPLS-AA force field for proteins via comparison with accurate quantum chemical calculations on peptides. J. Phys. Chem. B 105, 6474–6487.

Kiiskinen, L.-L., Viikari, L., Kruus, K., 2002. Purification and characterisation of a novel laccase from the ascomycete *Melanocarpus albomyces*. Appl. Microbiol. Biot. 59, 198–204.

Kitjaruwankul, S., Boonamnaj, P., Fuklang, S., Supunyabut, C., Sompornpisut, P., 2015. Shaping the water crevice to accommodate the voltage sensor in a down conformation: a molecular dynamics simulation study. J. Phys. Chem. B 119, 6516–6524.

Li, Z., Lazaridis, T., 2007. Water at biomolecular binding interfaces. Phys. Chem. Chem. Phys. 9, 573–581.

Liu, L., Zeng, Z., Zeng, G., Chen, M., Zhang, Y., Zhang, J., Fang, X., Jiang, M., Lu, L., 2012. Study on binding modes between cellobiose and beta-glucosidases from glycoside hydrolase family 1. Bioorg. Med. Chem. Lett. 22, 837–843.

Mashiach, E., Schneidman-Duhovny, D., Andrusier, N., Nussinov, R., Wolfson, H.J., 2008. FireDock: a web server for fast interaction refinement in molecular docking. Nucleic Acids Res. 36, W229–W232.

Mubarak, N., Wong, J., Tan, K., Sahu, J., Abdullah, E., Jayakumar, N., Ganesan, P., 2014. Immobilization of cellulase enzyme on functionalized multiwall carbon nanotubes. J. Mol. Catal. B Enzym. 107, 124–131.

Munk, L., Sitarz, A.K., Kalyani, D.C., Mikkelsen, J.D., Meyer, A.S., 2015. Can laccases catalyze bond cleavage in lignin? Biotechnol. Adv. 33, 13–24.

Mycroft, Z., Gomis, M., Mines, P., Law, P., Bugg, T.D., 2015. Biocatalytic conversion of lignin to aromatic dicarboxylic acids in *Rhodococcus jostii* RHA1 by re-routing aromatic degradation pathways. Green Chem. 17, 4974–4979.

Okai, M., Ohtsuka, J., Imai, L.F., Mase, T., Moriuchi, R., Tsuda, M., Nagata, K., Nagata, Y., Tanokura, M., 2013. Crystal structure and site-directed mutagenesis analyses of haloalkane dehalogenase LinB from *Sphingobium* sp. strain MI1205. J. Bacteriol. 195, 2642–2651.

Park, S., Vosguerichian, M., Bao, Z., 2013. A review of fabrication and applications of carbon nanotube film-based flexible electronics. Nanoscale 5, 1727–1752.

Pence, H.E., Williams, A., 2010. ChemSpider: an online chemical information resource. J. Chem. Educ. 87, 1123–1124.

Pronk, S., Páll, S., Schulz, R., Larsson, P., Bjelkmar, P., Apostolov, R., Shirts, M.R., Smith, J.C., Kasson, P.M., van der Spoel, D., Hess, B., Lindahl, E., 2013. GROMACS 4.5: a high-throughput and highly parallel open source molecular simulation toolkit. Bioinformatics 29, 845–854.

Ribeiro, A.A., Horta, B.A., Alencastro, R.B.D., 2008. MKTOP: a program for automatic construction of molecular topologies. J. Braz. Chem. Soc. 19, 1433–1435.

Rose, P.W., Bi, C., Bluhm, W.F., Christie, C.H., Dimitropoulos, D., Dutta, S., Green, R.K., Goodsell, D.S., Prlić, A., Quesada, M., 2013. The RCSB protein data bank: new resources for research and education. Nucleic Acids Res. 41, D475–D482.

Sánchez, C., 2009. Lignocellulosic residues: biodegradation and bioconversion by fungi. Biotechnol. Adv. 27, 185–194.

Salentin, S., Schreiber, S., Haupt, V.J., Adasme, M.F., Schroeder, M., 2015. PLIP: fully automated protein–ligand interaction profiler. Nucleic Acids Res. 43, W443–W447.

Schneidman-Duhovny, D., Inbar, Y., Nussinov, R., Wolfson, H.J., 2005. PatchDock and SymmDock: servers for rigid and symmetric docking. Nucleic Acids Res. 33, W363–W367.

Schomburg, I., Chang, A., Schomburg, D., 2002. BRENDA, enzyme data and metabolic information. Nucleic Acids Res. 30, 47–49.

Shulaker, M.M., Hills, G., Patil, N., Wei, H., Chen, H.-Y., Wong, H.-S.P., Mitra, S., 2013. Carbon nanotube computer. Nature 501, 526–530.

Shvedova, A.A., Pietroiusti, A., Fadeel, B., Kagan, V.E., 2012. Mechanisms of carbon nanotube-induced toxicity: focus on oxidative stress. Toxicol. Appl. Pharm. 261, 121–133.

Sun, Q., Xie, H.-B., Chen, J., Li, X., Wang, Z., Sheng, L., 2013. Molecular dynamics simulations on the interactions of low molecular weight natural organic acids with C 60. Chemosphere 92, 429–434.

Sundaramoorthy, M., Youngs, H.L., Gold, M.H., Poulos, T.L., 2005. High-resolution crystal structure of manganese peroxidase: substrate and inhibitor complexes. Biochemistry-U.S. 44, 6463–6470.

Tavares, A.P., Silva, C.G., Dražić, G., Silva, A.M., Loureiro, J.M., Faria, J.L., 2015. Laccase immobilization over multi-walled carbon nanotubes: kinetic, thermodynamic and stability studies. J. Colloid Interf. Sci. 454, 52–60.
Thomsen, R., Christensen, M.H., 2006. MolDock: a new technique for high-accuracy molecular docking. J. Med. Chem. 49, 3315–3321.
Torres, E., Bustos-Jaimes, I., Le Borgne, S., 2003. Potential use of oxidative enzymes for the detoxification of organic pollutants. Appl. Catal. B Environ. 46, 1–15.
Yamada, T., Hayamizu, Y., Yamamoto, Y., Yomogida, Y., Izadi-Najafabadi, A., Futaba, D.N., Hata, K., 2011. A stretchable carbon nanotube strain sensor for human-motion detection. Nat. Nanotechnol. 6, 296–301.
Yuan, S., Hu, Z., Filipek, S., Vogel, H., 2015. W2466. 48 opens a gate for a continuous intrinsic water pathway during activation of the adenosine A2A receptor. Angew. Chem. 127, 566–569.
Zhang, C., Chen, W., Alvarez, P.J., 2014. Manganese peroxidase degrades pristine but not surface-oxidized (carboxylated) single-walled carbon nanotubes. Environ. Sci. Technol. 48, 7918–7923.
Zhang, Y., Zeng, Z., Zeng, G., Liu, X., Chen, M., Liu, L., Liu, Z., Xie, G., 2013. Enzyme–Substrate binding landscapes in the process of nitrile biodegradation mediated by nitrile hydratase and amidase. Appl. Biochem. Biotech. 170, 1614–1623.
Zoppini, A., Ademollo, N., Amalfitano, S., Capri, S., Casella, P., Fazi, S., Marxsen, J., Patrolecco, L., 2016. Microbial responses to polycyclic aromatic hydrocarbon contamination in temporary river sediments: experimental insights. Sci. Total Environ. 541, 1364–1371.